Autler–Townes spectroscopy of high-lying state by phase conjugate six-wave mixing*

Jin-Hai Bai(白金海), Jian-Jun Li(李建军), Ling-An Wu(吴令安), Pan-Ming Fu(傅盘铭), Ru-Quan Wang(王如泉)†, and Zhan-Chun Zuo(左战春)‡

Laboratory of Optical Physics, Beijing National Laboratory for Condensed Matter Physics, Institute of Physics, Chinese Academy of Sciences, Beijing 100190, *China*

(Received 18 October 2016; revised manuscript received 29 November 2017; published online 10 March 2017)

An Autler–Townes (AT) spectroscopy based on phase conjugate six-wave mixing (SWM) is proposed to detect AT doublet of high-lying state in a Doppler-broadened cascade four-level system. It is found that the SWM spectrum is dependent strongly on the ratios between the magnitudes of the wave vectors. We discuss how the Doppler broadening affects the SWM spectrum from a time-domain viewpoint and find that, due the atomic motion, the atomic polarizations acquire different phases for atoms with different velocities as time evolves. The Doppler free SWM spectrum can be obtained only when the atomic polarization can be rephasing again at certain time after the interactions of all the incident fields.

Keywords: Autler–Townes splitting, six-wave mixing, Doppler broadening

PACS: 42.65.–k, 42.65.Dr, 42.50.Gy **DOI:** 10.1088/1674-1056/26/4/044204

1. Introduction

When a two-level system is driven by a strong coupling field of a resonant frequency, the populations of the states undergo coherent Rabi oscillations, as a result, there appears sidebands known as Autler–Townes (AT) doublet.[1] The AT doublet has been demonstrated in both atomic[2] and molecular systems,[3–5] as well in quantum dots[6–8] and in superconducting qubits.[9,10] One important application of the AT effect is to use it to measure the absolute value of the molecular transition dipole moment[3] and its internuclear distance dependence.[11] On the other hand, the effects of inhomogeneous Doppler line broadening on the AT splitting have been investigated.[12,13]

Traditionally, AT doublet was observed in three-level system, where the states are probed through a transition to or from a third level by probe absorption or fluorescence excitation spectroscopies. In this paper, we shall study the AT effect of high-lying state in a cascade four-level system. Our method is based on the generalized n-photon resonant $2n$-wave mixing with phase conjugation geometry, which is a general method to study the highly energy-state through monitoring the transition between the first excited state $|1\rangle$ and the ground state $|0\rangle$.[14] Since the transition $|1\rangle - |0\rangle$ is usually very strong, this spectroscopy can be very efficient. Previous, we have used six-wave mixing (SWM) to study the doubly excited autoionizing Rydberg states of Ba. Here, we shall used phase conjugate SWM to probe the AT doublet of high-lying state in a Doppler-broadened cascade four-level system. The critical role of Doppler broadening on the observation of AT splitting is investigated.

2. Basic theory

Let us consider a cascade four-level system (Fig. 1), where the states between $|0\rangle$ and $|1\rangle$, $|1\rangle$ and $|2\rangle$, and $|2\rangle$ and $|3\rangle$ are coupled by dipolar transitions with resonant frequencies Ω_1, Ω_2, and Ω_3, and dipole moment matrix elements μ_1, μ_2, and μ_3, respectively. In the phase conjugate SWM, beams 3 and 3′ have the same frequency ω_3 and a small angle exists between them. Beam 1 with frequency ω_1 propagates along the opposite direction of beam 3, while beam 2 with frequency ω_2 can propagate either along the direction of beam 3 or along the opposite direction.

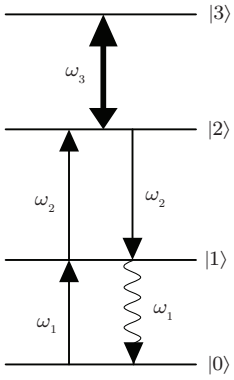


Fig. 1. Energy-level diagram for resonant SWM in a cascade four-level system.

*Project supported by the National Basic Research Program of China (Grant No. 2013CB922002), the National Natural Science Foundation of China (Grant Nos. 11274376 and 61308011), and the National High Technology Research and Development Program of China (Grant No. 2011AA120102).

†Corresponding author. E-mail: ruquanwang@iphy.ac.cn

‡Corresponding author. E-mail: zczuo@iphy.ac.cn

© 2017 Chinese Physical Society and IOP Publishing Ltd

Assuming that $\omega_i \simeq \Omega_i$ so that ω_i drives the transition from $|i-1\rangle$ to $|i\rangle$, the simultaneous interactions of atoms with beams 1, 2 to 3 will induce atomic coherence between $|0\rangle$ and $|3\rangle$ through resonant three-photon transition. This three-photon coherence is then probed by beams $3'$ and 2, and as a result an SWM signal of frequency ω_1 is generated almost opposite to the direction of beam $3'$.

Let the detunings be represented by $\Delta_i = \Omega_i - \omega_i$, so after a canonical transformation the effective Hamiltonian is the following

$$\begin{aligned} H = {} & \hbar\Delta_1|1\rangle\langle 1| + \hbar(\Delta_1+\Delta_2)|2\rangle\langle 2| \\ & + \hbar(\Delta_1+\Delta_2+\Delta_3)|3\rangle\langle 3| \\ & - \left[\mu_1 E_1|1\rangle\langle 0| + \mu_2 E_2|2\rangle\langle 1| \right. \\ & \left. + \mu_3 E_3|3\rangle\langle 2| + \text{H.c}\right], \end{aligned} \tag{1}$$

where E_i is the complex incident laser fields with frequency ω_i $(i = 1,2,3)$. The density matrix equations with relaxation terms included is given by

$$\frac{\mathrm{d}\rho}{\mathrm{d}t} = -\frac{\mathrm{i}}{\hbar}[H,\rho] + \left(\frac{\mathrm{d}\rho}{\mathrm{d}t}\right)_{\text{relax}}. \tag{2}$$

The nonlinear polarization responsible for the SWM signal is proportional to the off-diagonal density matrix element ρ_{10}. We shall consider the solution in the first and second order in E_1 and E_2, respectively, while to all order in E_3. This can be done by solving the following equations through perturbation

$$\begin{aligned} \frac{\mathrm{d}\rho_{10}}{\mathrm{d}t} = {} & -(\mathrm{i}\Delta_1 + \Gamma_{10})\rho_{10} + \mathrm{i}G_2^*\rho_{20} \\ & + \mathrm{i}G_1(\rho_{00} - \rho_{11}), \\ \frac{\mathrm{d}\rho_{20}}{\mathrm{d}t} = {} & -[\mathrm{i}(\Delta_1+\Delta_2) + \Gamma_{20}]\rho_{20} + \mathrm{i}G_2\rho_{10} \\ & + \mathrm{i}G_3^*\rho_{30}, \\ \frac{\mathrm{d}\rho_{30}}{\mathrm{d}t} = {} & -[\mathrm{i}(\Delta_1+\Delta_2+\Delta_3) + \Gamma_{30}]\rho_{30} \\ & + \mathrm{i}G_3\rho_{20}, \end{aligned} \tag{3}$$

where $G_i = \mu_i E_i/\hbar$ denote the coupling coefficients. The perturbation chain for SWM is

$$\rho_{00}^{(0)} \to \rho_{10}^{(1)} \to \rho_{20}^{(2)} \to \rho_{30}^{(3)} \to \rho_{20}^{(4)} \to \rho_{10}^{(5)}.$$

First, we have $\rho_{10}^{(1)} = \mathrm{i}G_1/(\mathrm{i}\Delta_1 + \Gamma_{10})$. On the other hand, since beam 3 is a strong field, which couple the states $|2\rangle$ and $|3\rangle$, we have to solve the following equations

$$-[\mathrm{i}(\Delta_1+\Delta_2)+\Gamma_{20}]\rho_{20} + \mathrm{i}G_3^*\rho_{30} = -\mathrm{i}G_2\rho_{10}^{(1)} - [\mathrm{i}(\Delta_1+\Delta_2+\Delta_3)+\Gamma_{30}]\rho_{30} + \mathrm{i}G_3\rho_{20} = 0, \tag{4}$$

and obtain

$$\rho_{20} = \frac{-G_1G_2\Gamma_{30}^{\mathrm{c}}}{\Gamma_{10}^{\mathrm{c}}(\Gamma_{20}^{\mathrm{c}}\Gamma_{30}^{\mathrm{c}} + |G_3|^2)}, \tag{5}$$

where $\Gamma_{10}^{\mathrm{c}} = \Gamma_{10} + \mathrm{i}\Delta_1$, $\Gamma_{20}^{\mathrm{c}} = \Gamma_{20} + \mathrm{i}(\Delta_1+\Delta_2)$, and $\Gamma_{30}^{\mathrm{c}} = \Gamma_{30} + \mathrm{i}(\Delta_1+\Delta_2+\Delta_3)$. Finally, from $\rho_{10} = \mathrm{i}G_2^*\rho_{20}/\Gamma_{10}^{\mathrm{c}}$, we obtain the density matrix element ρ_{10} responsible for the SWM

$$\rho_{10} = \frac{-\mathrm{i}G_1|G_2|^2\Gamma_{30}^{\mathrm{c}}}{(\Gamma_{10}^{\mathrm{c}})^2(\Gamma_{20}^{\mathrm{c}}\Gamma_{30}^{\mathrm{c}} + |G_3|^2)}. \tag{6}$$

Now, we consider the special case of SWM with phase conjugation geometry. Equation (6) contains the contribution from FWM, i.e.,

$$\rho_{10}^{\mathrm{FWM}} = \rho_{10}(|G_3| = 0) = -\mathrm{i}G_1|G_2|^2/(\Gamma_{10}^{\mathrm{c}})^2\Gamma_{20}^{\mathrm{c}}. \tag{7}$$

By subtracting this term, we obtain

$$\begin{aligned} \rho_{10}^{(5)} = {} & \rho_{10}(|G_3|) - \rho_{10}^{\mathrm{FWM}} \\ = {} & \frac{\mathrm{i}|G_1||G_2|^2|G_3|^2}{(\Gamma_{10}^{\mathrm{c}})^2\Gamma_{20}^{\mathrm{c}}(\Gamma_{20}^{\mathrm{c}}\Gamma_{30}^{\mathrm{c}} + |G_3|^2)}. \end{aligned} \tag{8}$$

We then consider the phase-matching condition. Let the complex incident laser fields be written as $E_i = \varepsilon_i \mathrm{e}^{\mathrm{i}\boldsymbol{k}_i\cdot\boldsymbol{r}}$ $(i = 1,2)$ while $E_3 = \varepsilon_3 \mathrm{e}^{\mathrm{i}\boldsymbol{k}_3\cdot\boldsymbol{r}} + \varepsilon_3' \mathrm{e}^{\mathrm{i}\boldsymbol{k}_3'\cdot\boldsymbol{r}}$, where $\boldsymbol{k}_i$ and $\boldsymbol{k}_3'$ are the wave vectors of beams i and $3'$, respectively, then $G_i(\boldsymbol{r}) = g_i \mathrm{e}^{\mathrm{i}\boldsymbol{k}_i\cdot\boldsymbol{r}}$ $(i = 1,2)$ and $G_3(\boldsymbol{r}) = g_3 \mathrm{e}^{\mathrm{i}\boldsymbol{k}_3\cdot\boldsymbol{r}} + g_3' \mathrm{e}^{\mathrm{i}\boldsymbol{k}_3'\cdot\boldsymbol{r}}$, with $g_i = \mu_i\varepsilon_i/\hbar$ $(i = 1,2,3)$ and $g_3' = \mu_3\varepsilon_3'/\hbar$. In the following discussions we assume that $g_3 \gg g_3'$, then the corresponding off-diagonal density matrix element for SWM is given by

$$\rho_{10}^{\mathrm{SWM}}(\boldsymbol{r}) = \frac{\mathrm{i}S(\boldsymbol{r})}{(\Gamma_{10}^{\mathrm{c}})^2\Gamma_{20}^{\mathrm{c}}(\Gamma_{20}^{\mathrm{c}}\Gamma_{30}^{\mathrm{c}} + |g_3|^2)}, \tag{9}$$

where

$$S(\boldsymbol{r}) = g_1|g_2|^2 g_3(g_3')^* \mathrm{e}^{\mathrm{i}(\boldsymbol{k}_1+\boldsymbol{k}_3-\boldsymbol{k}_3')\cdot\boldsymbol{r}},$$

and the SWM signal propagates along the direction $\boldsymbol{k}_1 + \boldsymbol{k}_3 - \boldsymbol{k}_3'$.

Let us now consider the Doppler effect. The nonlinear polarization $P^{\mathrm{NL}}(\boldsymbol{r})$ responsible for the SWM signal is given by averaging over the velocity distribution function $W(\boldsymbol{v})$, i.e.,

$$P^{\mathrm{NL}}(\boldsymbol{r}) = N\mu_1 \int_{-\infty}^{\infty} \mathrm{d}\boldsymbol{v}\ W(\boldsymbol{v})\rho_{10}^{\mathrm{SWM}}(\boldsymbol{r},\boldsymbol{v}). \tag{10}$$

Here $\rho_{10}^{\mathrm{SWM}}(\boldsymbol{r},\boldsymbol{v})$ is obtained from Eq. (9) by using the Doppler-shift frequency detunings, i.e., $\Delta_i^{\mathrm{d}} = \Delta_i + \boldsymbol{k}_i\cdot\boldsymbol{v}$ $(i = 1,2,3)$ and $\Delta_3'^{\mathrm{d}} = \Delta_3 + \boldsymbol{k}_3'\cdot\boldsymbol{v}$, N is the density of the atoms, while

$$W(\boldsymbol{v}) = \frac{1}{\sqrt{\pi}u}\exp\left[-(v/u)^2\right], \tag{11}$$

where $u=\sqrt{2KT/m}$ with m being the mass of an atom, K is Boltzmann's constant, and T the absolute temperature. The SWM signal intensity is proportional to $|P^{\rm NL}|^2$.

3. Autler–Townes splitting in six-wave mixing spectrum

In this section, we shall study how the AT effect affects the SWM spectrum in a Doppler-broadened system. For comparison, we start with the homogeneously broadened system. The resonant condition can obtain by solving the pole structure in Eq. (9), i.e.,

$$[(\Delta_1+\Delta_2)-{\rm i}\Gamma_{20}][(\Delta_1+\Delta_2+\Delta_3)-{\rm i}\Gamma_{30}]-|g_3|^2=0. \quad (12)$$

When we scan Δ_2 with $\Delta_1=\Delta_3=0$, the SWM spectrum is given by

$$\rho_{10}^{\rm SWM}(\Delta_2)\propto\frac{-1}{(\Delta_2-{\rm i}\Gamma_{20})(\Delta_2-\Delta_+)(\Delta_2-\Delta_-)}, \quad (13)$$

where

$$\Delta_\pm=\frac{1}{2}\left[{\rm i}(\Gamma_{20}+\Gamma_{30})\pm\sqrt{4|g_3|^2-(\Gamma_{20}+\Gamma_{30})^2}\right]. \quad (14)$$

It shows that the resonances occur at $\Delta_2=0$ and $\Delta_2\simeq\pm|g_3|$ when $|g_3|\gg(\Gamma_{20}+\Gamma_{30})/2$. On the other hand, if we scan Δ_1 with $\Delta_2=\Delta_3=0$, then the SWM spectrum becomes

$$\rho_{10}^{\rm SWM}(\Delta_1)\propto\frac{1}{(\Delta_1-{\rm i}\Gamma_{10})^2(\Delta_1-{\rm i}\Gamma_{20})}\times\frac{1}{(\Delta_1-\Delta_+)(\Delta_1-\Delta_-)}, \quad (15)$$

where again the resonances occur at $\Delta_1=0$ and $\Delta_1\simeq\pm|g_3|$.

Now, we investigate the AT splitting in the SWM spectrum in a Doppler-broadened system. We assume that beam 2 propagates along the direction of beam 3, so $\boldsymbol{k}_1=-k_1\boldsymbol{z}$, $\boldsymbol{k}_2=k_2\boldsymbol{z}$ and $\boldsymbol{k}_3=k_3\boldsymbol{z}$, while $\boldsymbol{k}_3'$ is approximated as $\boldsymbol{k}_3'\simeq k_3\boldsymbol{z}$ because the angle between beams 3 and 3′ is typically very small. We express $\rho_{10}^{\rm SWM}$ in Eq. (10) as a function of v explicitly, then

$$\rho_{10}^{\rm SWM}(v)=\frac{\eta}{(v-\tilde{\Delta}_{10})^2(v-\tilde{\Delta}_{20})}\times\frac{1}{(v-\tilde{\Delta}_{20})(v-\tilde{\Delta}_{30})-|\tilde{g}_3|^2}, \quad (16)$$

where

$$\begin{aligned}&\tilde{\Delta}_{10}=(\Delta_1-{\rm i}\Gamma_{10})/k_1,\\&\tilde{\Delta}_{20}=(\Delta_1+\Delta_2-i\Gamma_{20})/k_1(1-\zeta_2),\\&\tilde{\Delta}_{30}=(\Delta_1+\Delta_2+\Delta_3-{\rm i}\Gamma_{30})/k_1(1-\zeta_2-\zeta_3),\\&|\tilde{g}_3|^2=|g_3|^2/k_1^2(1-\zeta_2)(1-\zeta_2-\zeta_3),\\&\eta=-S/[k_1^5(1-\zeta_2)^2(1-\zeta_2-\zeta_3)],\end{aligned}$$

with $\zeta_2=k_2/k_1$ and $\zeta_3=k_3/k_1$ the ratios between the magnitudes of the wave vectors. By solving the pole structure in Eq. (16), i.e.,

$$(v-\tilde{\Delta}_{20})(v-\tilde{\Delta}_{30})-|\tilde{g}_3|^2=0, \quad (17)$$

we obtain

$$\rho_{10}^{\rm SWM}(v)=\frac{\eta}{(v-\tilde{v}_1)^2(v-\tilde{v}_2)(v-\tilde{v}_+)(v-\tilde{v}_-)}, \quad (18)$$

where

$$\begin{aligned}\tilde{v}_1&=\tilde{\Delta}_{10},\\\tilde{v}_2&=\tilde{\Delta}_{20},\\\tilde{v}_\pm&=\frac{1}{2}(\tilde{\Delta}_{20}+\tilde{\Delta}_{30})\\&\quad\pm(1/2)\sqrt{(\tilde{\Delta}_{20}-\tilde{\Delta}_{30})^2+4|\tilde{g}_3|^2}.\end{aligned} \quad (19)$$

Therefore, we have

$$P^{\rm NL}\propto\int_{-\infty}^{\infty}{\rm d}v\ \frac{{\rm e}^{-(v/u)^2}}{(v-\tilde{v}_1)^2(v-\tilde{v}_2)(v-\tilde{v}_+)(v-\tilde{v}_-)}. \quad (20)$$

$\rho_{10}^{\rm SWM}(v)$ in Eq. (18) has four poles, i.e., $\tilde{v}_1$, $\tilde{v}_2$, and $\tilde{v}_\pm$, and the integral in Eq. (20) consists mainly of the contributions of atoms with velocities $v\simeq v_1$, $v\simeq v_2$, and $v\simeq v_\pm$, which vary as we scan the incident laser frequencies Δ_i. Here, v_1, v_2, and $v_\pm$ are the real parts of $\tilde{v}_1$, $\tilde{v}_2$, and $\tilde{v}_\pm$, respectively. Considering the case that v_1, v_2, $v_\pm\ll u$, then, since $\tilde{v}_1$ is a pole of second order, the resonance of $P^{\rm NL}$ appears when $v_2=v_1$ or $v_\pm=v_1$.

We neglect the relaxation rates and define

$$\begin{aligned}&\Delta_{10}=\Delta_1/k_1,\\&\Delta_{20}=(\Delta_1+\Delta_2)/k_1(1-\zeta_2),\\&\Delta_{30}=(\Delta_1+\Delta_2+\Delta_3)/k_1(1-D-\zeta_3).\end{aligned}$$

Then, for the resonant condition $v_2=v_1$, we have

$$\zeta_2\Delta_1=-\Delta_2. \quad (21)$$

On the other hand, for $v_\pm=v_1$ we have

$$\frac{\Delta_1}{k_1}=\frac{1}{2}\left[(\Delta_{20}+\Delta_{30})\pm\sqrt{(\Delta_{20}-\Delta_{30})^2+4|\tilde{g}_3|^2}\right]. \quad (22)$$

Now, we study the spectra of scanning Δ_1 and Δ_2 separately. First, let us consider the spectrum of Δ_2 with $\Delta_1=\Delta_3=0$. According to Eqs. (21) and (22), the resonances are given by $\Delta_2=0$ and $\pm|g_3|$, respectively. This spectrum is the same as that in the homogeneously broadened system. Next, we consider the spectrum of Δ_1 with $\Delta_2=\Delta_3=0$. Unlike the spectrum of Δ_2, it is found that the resonance conditions become $\Delta_1=0$ and $\Delta_1=\pm|g_3|/\sqrt{\zeta_2(\zeta_2+\zeta_3)}$, which depends on the ratios between the magnitudes of the wave vectors.

4. Numerical results

In this section we shall present numerical results of SWM spectra in a cascade four-level system with parameters $\Gamma_{10}/\Gamma_{30} = \Gamma_{20}/\Gamma_{30} = 0.2$. Let us start with the homogeneously broadened case. Figures 2(a) and 2(b) present the SWM intensity versus Δ_1 and Δ_2, respectively, with $\Delta_3/\Gamma_{30} = 0$, $g_3/\Gamma_{30} = 0.1$ (solid curve), 5 (dashed curve), and 10 (dash–dotted curve), while $\Delta_2/\Gamma_{30} = 0$ for panel (a) and $\Delta_1/\Gamma_{30} = 0$ for panel (b). When Δ_2 is scanned, we observe three peaks with AT splitting appears at $\Delta_2 = \pm|g_3|$ [see Fig. 2(b)]. By contrast, there is only single peak at $\Delta_1 = 0$ when we scan Δ_1 [Fig. 2(a)]. To understand these spectra, we consider the limit $|g_3| \gg \Gamma_{10}, \Gamma_{20}, \Gamma_{30}$ for simplicity. For the SWM spectrum of Δ_1, we have

$$I(|g_3|)/I(0) = \Gamma_{10}^4\Gamma_{20}^2/[(\Gamma_{20}+\Gamma_{30})^2|g_3|^4],$$

which is much less than 1. On the other hand, for the spectrum of Δ_2, we have

$$I(|g_3|)/I(0) = \Gamma_{20}^2/[(\Gamma_{20}+\Gamma_{30})^2.$$

Physically, for the spectrum of Δ_1, the peaks at $\Delta_1 = 0$ and at $\Delta_1 = \pm|g_3|$ correspond to the one-photon transition between states $|0\rangle$ and $|1\rangle$ and two-photon transition from $|0\rangle$ to the dressed states, respectively, leading to the fact that the signal of the former is much larger than that of the latter.

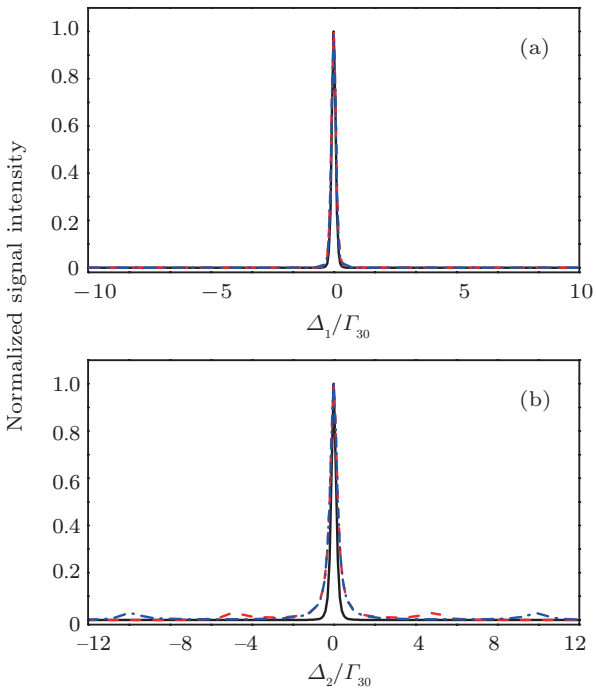


Fig. 2. (color online) SWM intensity versus (a) Δ_1 and (b) Δ_2 in a homogeneously broadened system with parameters $\Delta_3/\Gamma_{30} = 0$ and $g_3/\Gamma_{30} = 0.1$ (solid curve), 5 (dashed curve), and 10 (dash–dotted curve), while $\Delta_2/\Gamma_{30} = 0$ for panel (a) and $\Delta_1/\Gamma_{30} = 0$ for panel (b).

Now, let us consider the SWM spectra in a Doppler-broadened system with $\Gamma_{30}/k_1u = 0.02$. Figures 3(a) and 3(b) present the SWM intensity versus Δ_1 and Δ_2, respectively, when $\zeta_2 = \zeta_3 = 1.2$, $\Delta_3/\Gamma_{30} = 0$ and $g_3/\Gamma_{30} = 0.1$ (solid curve), 5 (dashed curve), and 10 (dash–dotted curve), while $\Delta_2/\Gamma_{30} = 0$ for panel (a) and $\Delta_1/\Gamma_{30} = 0$ for panel (b). First of all, these spectra are Doppler-free. Moreover, the SWM spectra of scanning Δ_2 [Fig. 3(b)] are similar to those in the homogeneously broadened case [Fig. 2(b)] in which there exists three peaks with AT splitting appears at $\Delta_2 = \pm|g_3|$. By contrast, unlike the corresponding case in the homogeneously broadened system the SWM spectra of Δ_1 [Fig. 3(a)] exhibits three peaks also with AT splitting appears at

$$\Delta_1 = \pm|g_3|/\sqrt{\zeta_2(\zeta_2+\zeta_3)}.$$

Physically, the peak at $\Delta_1 = 0$ is derived from the condition $v_1 = v_2$, while the AT splitting from the condition $v_1 = v_\pm$. Since there are of the same order, leading to the simultaneous appearance of three peaks in both the SWM spectra of Δ_1 and Δ_2.

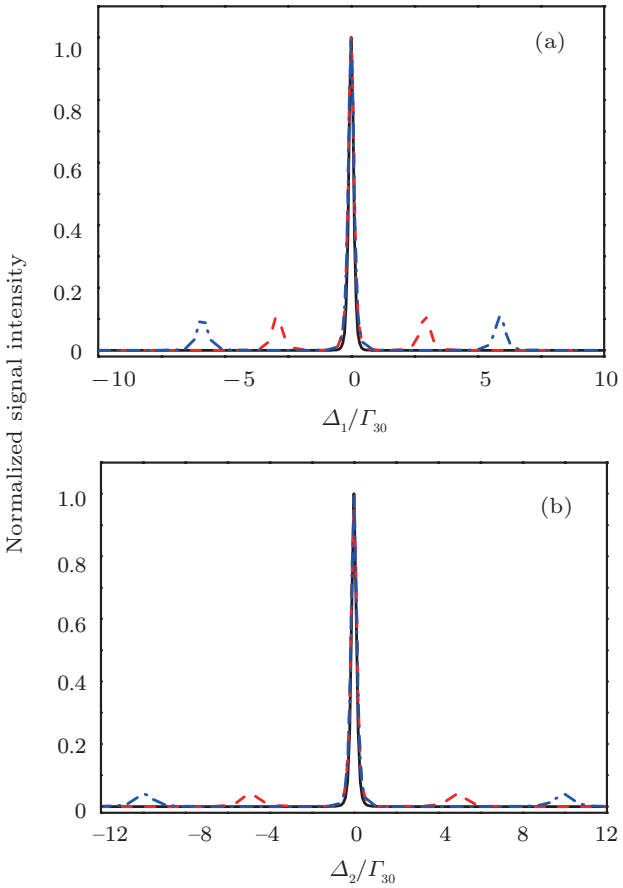


Fig. 3. (color online) SWM intensity versus (a) Δ_1 and (b) Δ_2 in a Doppler-broadened system with $\zeta_2 = \zeta_3 = 1.2$ when $\Delta_3/\Gamma_{30} = 0$ and $g_3/\Gamma_{30} = 0.1$ (solid curve), 5 (dashed curve), and 10 (dash–dotted curve), while $\Delta_2/\Gamma_{30} = 0$ for panel (a) and $\Delta_1/\Gamma_{30} = 0$ for panel (b).

Now, we consider another Doppler-broadened case with $\zeta_2 = \zeta_3 = 0.4$. Figures 4(a) and 4(b) present the SWM intensity versus Δ_1 and Δ_2, respectively, when $\Delta_3/\Gamma_{30} = 0$ and $g_3/\Gamma_{30} = 0.1$ (solid curve), 50 (dashed curve), and 100 (dash–dotted curve), while $\Delta_2/\Gamma_{30} = 0$ for panel (a) and $\Delta_1/\Gamma_{30} = 0$ for panel (b). Unlike the previous cases, the SWM spectrum

is extremely broad. Physically, the broadening is due the polarization interference between atoms of different velocities, as we shall discuss in the next section. This can be verified through artificially ignoring the polarization interference by calculating

$$\int_{-\infty}^{\infty} \mathrm{d}v \ \ \mathrm{e}^{-(v/u)^2} |\rho_{10}(r,v)|^2.$$

The dotted curves in Figs. 4(a) and 4(b) present the results with $g_3/\Gamma_{30} = 0.1$, which show again very narrow peaks, indicating that the broadening of the SWM spectrum is due to the polarization interference.

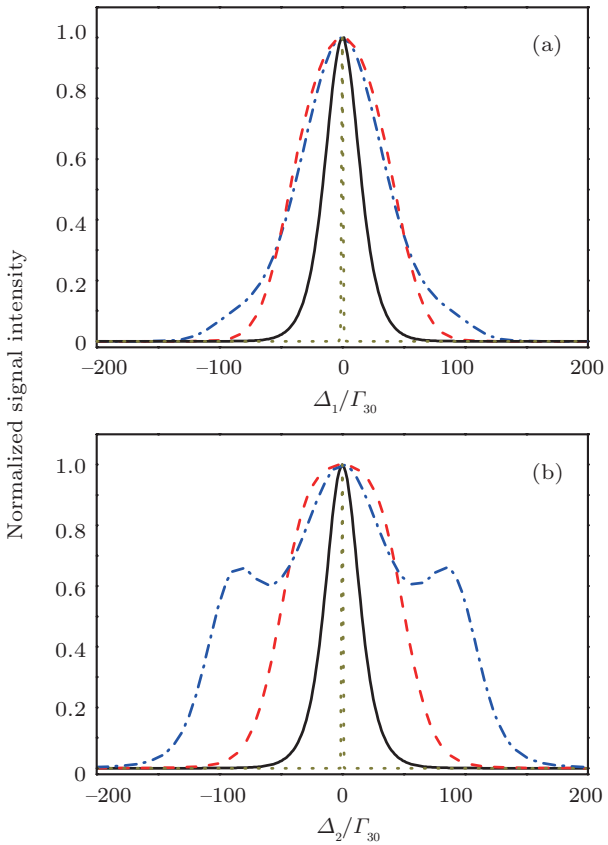


Fig. 4. (color online) SWM intensity versus (a) Δ_1 and (b) Δ_2 in a Doppler-broadened system with $\zeta_2 = \zeta_3 = 0.4$ when $\Delta_3/\Gamma_{30} = 0$ and $g_3/\Gamma_{30} = 0.1$ (solid curve), 50 (dashed curve), and 100 (dash–dotted curve), while $\Delta_2/\Gamma_{30} = 0$ for panel (a) and $\Delta_1/\Gamma_{30} = 0$ for panel (b). The dotted curves in panels (a) and (b) are the results for $g_3/\Gamma_{30} = 0.1$ when the polarization interference are ignored.

Finally, let us consider the case with $\zeta_2 = 0.8$ and $\zeta_3 = 0.4$. Figures 5(a) and 5(b) presents the SWM intensity versus Δ_1 and Δ_2, respectively, when $\Delta_3/\Gamma_{30} = 0$ and $g_3/\Gamma_{30} = 0.1$ (solid curve), 10 (dashed curve), and 20 (dash–dotted curve), while $\Delta_2/\Gamma_{30} = 0$ for panel (a) and $\Delta_1/\Gamma_{30} = 0$ for panel (b). Here, we observe a quite different SWM spectrum with only two narrow peaks with the central peak disappeared. These spectra are similar to the conventional AT spectrum in the three-level system.

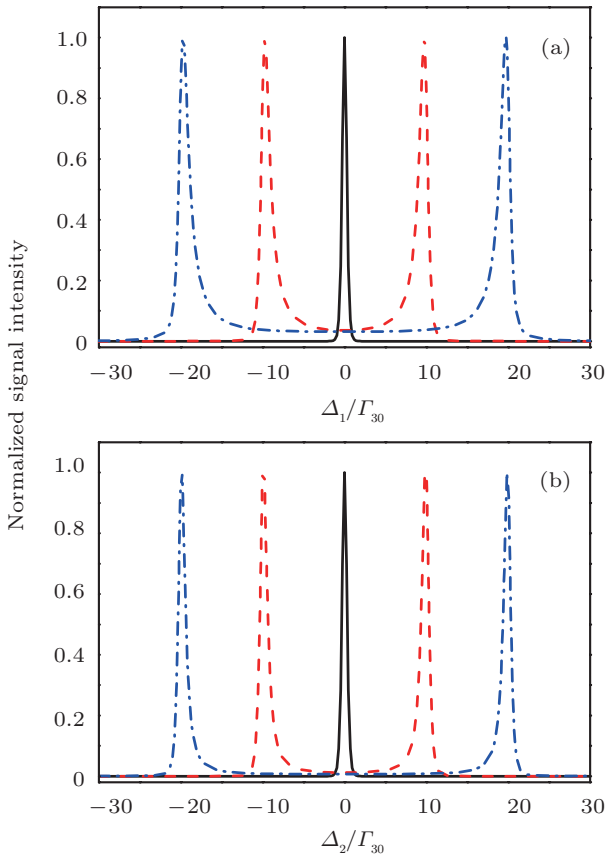


Fig. 5. (color online) SWM intensity versus (a) Δ_1 and (b) Δ_2 in a Doppler-broadened system with $\zeta_2 = 0.8$ and $\zeta_3 = 0.4$ when $\Delta_3/\Gamma_{30} = 0$ and $g_3/\Gamma_{30} = 0.1$ (solid curve), 10 (dashed curve), and 20 (dash–dotted curve), while $\Delta_2/\Gamma_{30} = 0$ for panel (a) and $\Delta_1/\Gamma_{30} = 0$ for panel (b).

5. The polarization interference in Doppler-broadened system

In this section we shall study how the polarization interference affects the phase conjugate SWM spectroscopy in a Doppler-broadened system. Let us compare the polarizations corresponding to the linear absorption (L), FWM and SWM in a Doppler-broadened system, which, from the perturbation theory, are given by

$$P^{\mathrm{L}} = \mathrm{i}N\mu_1 \int_{-\infty}^{\infty} \mathrm{d}v W(v) \int_0^{\infty} \mathrm{d}\tau G_1(t-\tau)\,\mathrm{e}^{-\Gamma_{10}^{\mathrm{d}}\tau}, \quad (23)$$

$$\begin{aligned} P^{\mathrm{FWM}} = -\mathrm{i}N\mu_1 \int_{-\infty}^{\infty} \mathrm{d}v W(v) \int_0^{\infty}\int_0^{\infty}\int_0^{\infty} \mathrm{d}\tau_1\,\mathrm{d}\tau_2\,\mathrm{d}\tau_3 \\ \times G_1(t-\tau_1-\tau_2-\tau_3) G_2(t-\tau_2-\tau_3) \\ \times G_2^*(t-\tau_3)\,\mathrm{e}^{-\Gamma_{10}^{\mathrm{d}}(\tau_1+\tau_3)}\,\mathrm{e}^{-\Gamma_{20}^{\mathrm{d}}\tau_2}, \end{aligned} \quad (24)$$

and

$$\begin{aligned} P^{\mathrm{SWM}} = \mathrm{i}N\mu_1 \int_{-\infty}^{\infty} \mathrm{d}v W(v) \int_0^{\infty}\int_0^{\infty}\cdots\int_0^{\infty} \mathrm{d}\tau_1\,\mathrm{d}\tau_2\cdots\mathrm{d}\tau_5 G_1(t-\tau_1-\tau_2-\tau_3-\tau_4-\tau_5) \\ \times G_2(t-\tau_2-\tau_3-\tau_4-\tau_5) G_3(t-\tau_3-\tau_4-\tau_5)\left[G_3'(t-\tau_4-\tau_5)\right]^* G_2^*(t-\tau_5)\,\mathrm{e}^{-\Gamma_{10}^{\mathrm{d}}(\tau_1+\tau_5)}\,\mathrm{e}^{-\Gamma_{20}^{\mathrm{d}}(\tau_2+\tau_4)}\,\mathrm{e}^{-\Gamma_{30}^{\mathrm{d}}\tau_3}, \end{aligned} \quad (25)$$

respectively. These equations show the time sequence of the interaction with different fields.

We start with the linear absorption, where atoms with velocity v interact the field G_1 at time $t-\tau$. Since $\boldsymbol{r}(t') = \boldsymbol{r}(t) - (t-t')\boldsymbol{v}$, we have $G_1(t-\tau)$ in Eq. (23) given by $G_1(t-\tau) \propto \mathrm{e}^{-\mathrm{i}k_1 v\tau}$, i.e., atoms with velocity v will acquire a relative phase $k_1 v\tau$ in a time interval τ, causing dephasing between atoms of different velocities. More specifically, after integrating over the velocity distribution function $W(\boldsymbol{v})$ we obtain a term $\mathrm{e}^{-(k_1 u/2)^2\tau^2}$. In other words, atoms excited during the time interval $\tau \sim 2/(k_1 u)$ will contribute to the linear absorption, leading to the Doppler broadening of the line shape.

Now, we turn to the FWM with incident beams given by $G_1(\boldsymbol{r}) = g_1\,\mathrm{e}^{\mathrm{i}\boldsymbol{k}_1\cdot\boldsymbol{r}}$ and $G_2(\boldsymbol{r}) = g_2\,\mathrm{e}^{\mathrm{i}\boldsymbol{k}_2\cdot\boldsymbol{r}}$, where $\boldsymbol{k}_1 = -k_1\boldsymbol{z}$ and $\boldsymbol{k}_2 = k_2\boldsymbol{z}$. As is well known, FWM is intrinsically Doppler-free when the incident beams have narrow linewidth, because if beam 1 with frequency ω_1 is within the Doppler profile of the transition from $|0\rangle$ to $|1\rangle$, then only atoms in a specific velocity group will contribute to the signal. However, the polarization interference can cause the FWM spectrum extremely broad. Specifically, atoms with velocity v interact with the fields G_1, G_2, and G_2^* at times $t-\tau_1-\tau_2-\tau_3$, $t-\tau_2-\tau_3$, and $t-\tau_3$, so the atomic polarizations acquire phases $-k_1 v(\tau_1+\tau_2+\tau_3)$, $\zeta_2 k_1 v(\tau_2+\tau_3)$, and $-\zeta_2 k_1 v\tau_3$, respectively, at each interaction. As a result, we have $G_1(t-\tau_1-\tau_2-\tau_3)G_2(t-\tau_2-\tau_3)G_2^*(t-\tau_3) \propto \mathrm{e}^{\mathrm{i}k_1 v[(\tau_1+\tau_3)-(\zeta_2-1)\tau_2]}$. Physically, there is dephasing between atoms of different velocities after the first field G_1. However, the subsequent interactions with fields G_2 and G_2^* can induce rephasing process, and then, cause constructive interference between atoms of different velocities if $\zeta_2 > 1$. In this case, the FWM signal originates mainly from the moments when the complete rephasing occurs, i.e., $(\tau_1+\tau_3)-(\zeta_2-1)\tau_2 = 0$. In other words, we can obtain a Doppler free FWM spectrum when $\zeta_2 > 1$. Otherwise, the randomization of the phases of the atomic polarizations will cause additional broadening of the spectrum line.[15–17]

Finally, we turn to the SWM. Atoms with velocity v interact with the fields G_1, G_2, G_3, $(G_3')^*$, and $(G_2)^*$ at times $t-\tau_1-\tau_2-\tau_3-\tau_4-\tau_5$, $t-\tau_2-\tau_3-\tau_4-\tau_5$, $t-\tau_3-\tau_4-\tau_5$, $t-\tau_4-\tau_5$, and $t-\tau_5$ so the atomic polarizations acquire phases $-k_1 v(\tau_1+\tau_2+\tau_3+\tau_4+\tau_5)$, $\zeta_2 k_1 v(\tau_2+\tau_3+\tau_4+\tau_5)$, $\zeta_3 k_1 v(\tau_3+\tau_4+\tau_5)$, $-\zeta_3 k_1 v(\tau_4+\tau_5)$, and $-\zeta_2 k_1 v\tau_5$, respectively, at each interaction. As a result, we have $G_1 G_2 G_3 (G_3')^* G_2^* \propto \mathrm{e}^{\mathrm{i}k_1 v[(\tau_1+\tau_5)+(1-\zeta_2)(\tau_2+\tau_4)+(1-\zeta_2-\zeta_3)\tau_5]}$. The complete rephasing occurs when $(\tau_1+\tau_5)+(1-\zeta_2)(\tau_2+\tau_4)+(1-\zeta_2-\zeta_3)\tau_5 = 0$, which can be satisfied if $\zeta_2+\zeta_3 > 1$. In other words, the SWM spectrum is Doppler free only when $\zeta_2+\zeta_3 > 1$, otherwise, the SWM spectrum becomes extremely broad.

Now, we investigate how the polarization interference affects the phase conjugate SWM spectrum. According to Eq. (8) the contribution to SWM signal consists of two components, i.e., an SWM term shown in Eq. (6) and an FWM term shown in Eq. (7), corresponding to the AT splitting and the central peak in the SWM spectrum, respectively. The polarization interference can have different effects on these two terms according to the values of ζ_2 and ζ_3. Let us first consider the case when $\zeta_2 > 1$. In this case the polarizations of both the FWM term and the SWM term can be rephasing completely, leading to the appearance of three resonant peaks with Doppler-free linewidth in the SWM spectrum, as shown in Fig. 3. Now let consider the case of $\zeta_2 < 1$. If $\zeta_2+\zeta_3 < 1$ simultaneously, then the phases of the polarizations of both the FWM term and the SWM term are randomized, so we obtain a extremely broadening of the SWM spectrum [see Fig. 4]. On the other hand, if $\zeta_2+\zeta_3 > 1$ then since the SWM term has narrow linewidth while the FWM term is so broad that its peak value is greatly reduced, as a result, the SWM spectrum exhibits only two narrow peaks corresponding to the AT doublet.

6. Conclusion

In this paper, we propose an AT spectroscopy based on phase conjugate SWM to detect AT doublet of high-lying state in a Doppler broadened cascade four-level system. This is important because it can be used to measure the dipole moment between the transition of highly excited states. It is worth mentioning that AT splitting have been observed previously by multi-wave mixing. For example, AT splitting of FWM[18] and SWM[19] have been demonstrated in electromagnetically induced transparency atomic media. However, in most previous works AT doublet was observed in low-lying state. By contrast, our work is concentrated on the AT doublet of high-lying states. The advantages of our method are the following. Compared to the method of detecting fluorescence from excited states, our scheme is still realizable even when state $|2\rangle$ or $|3\rangle$ has long radiative lifetimes so that direct detection of the fluorescence is difficult. This is because transitions between these states are driven by lasers, and so long as $|1\rangle$ to $|0\rangle$ is a strongly coupled transition, the wave-mixing signal can be emitted via this strong transition.

We also discussed the effect of Doppler broadening on the SWM spectrum from a time-domain viewpoint. Although this subject has been discussed in Refs. [15] and [16], here we concentrate on the physics underlying. Specifically, due the atomic motion, the atomic polarizations acquire different phases for atoms with different velocities as time evolves. The Doppler free SWM spectrum can be obtained only when the atomic polarization can be rephasing again at certain time after the interactions of all the incident fields.

References

[1] Autler S H and Townes C H 1955 *Phys. Rev.* **100** 703

[2] Fulton D J, Shepherd S, Moseley R R, Sinclair B D and Dunn M H 1995 *Phys. Rev. A* **5**2 2302

[3] Qi J, Spano F C, Kirova T, Lazoudis A, Magnes J, Li L, Narducci L M, Field R W and Lyyra A M 2002 *Phys. Rev. Lett.* **8**8 173003

[4] Qi J, Lazarov G, Wang X, Li L, Narducci L M, Lyyra A M and Spano F C 1999 *Phys. Rev. Lett.* **8**3 288

[5] Garcia-Fernandez R, Ekers A, Klavins J, Yatsenko L P, Bezuglov N N, Shore B W and Bergmann K 2005 *Phys. Rev. A* **7**1 023401

[6] Xu X D, Sun B, Berman P R, Steel D G, Bracker A S, Gammon D and Sham L J 2007 *Science* **3**17 929

[7] Vamivakas A N, Zhao Y, Lu C Y and Atatüre M 2009 *Nat. Phys.* **5** 198

[8] Muller A, Flagg E B, Bianucci P, Wang X Y, Deppe D G, Ma W, Zhang J, Salamo G J, Xiao M and Shih C K 2007 *Phys. Rev. Lett.* **9**9 187402

[9] Baur M, Filipp S, Bianchetti R, Fink J M, Göppl M, Steffen L, Leek P J, Blais A and Wallraff A 2009 *Phys. Rev. Lett.* **1**02 243602

[10] Sillanpää M A, Li J, Cicak K, Altomare F, Park J I, Simmonds R W, Paraoanu G S and Hakonen P J 2009 *Phys. Rev. Lett.* **1**03 193601

[11] Ahmed E H, Qi P, Beser B, Bai J, Field R W, Huennekens J P and Lyyra A M 2008 *Phys. Rev. A* **7**7 053414

[12] Ahmed E and Lyyra A M 2007 *Phys. Rev. A* **7**6 053407

[13] Niu J, Pei L, Lu X, Wang R, Wu L A and Fu P 2011 *Phys. Rev. A***8**4 033853

[14] Zuo Z, J Sun, Liu X, Jiang Q, Fu G, Wu L A and Fu P 2006 *Phys. Rev. Lett.* **9**7 193904

[15] Niu J, Wang R, Wu L A and Fu P 2009 *J. Opt. Soc. Am. B* **2**6 2268

[16] Niu J, Wang R, Wang B, Wu L A and Fu P 2009 *J. Phys. B: At. Mol. Opt. Phys.* **4**2 175505

[17] Li C, Zhang Y, Wang Z, Li Y, Nie Z, Zhao Y, Wang R, Yuan C and Lu K 2011 *Opt. Commun.* **2**84 1379

[18] Zhang Y, Nie Z, Wang Z, Li C, Wen F and Xiao M 2010 *Opt. Lett.* **3**5 3420

[19] Zhang Y, Li P, Zheng H, Wang Z, Chen H, Li C, Zhang R and Xiao M 2011 *Opt. Express* **1**9 7769